ELSEVIER

Solid State Ionics 146 (2002) 211–217

SOLID STATE IONICS

www.elsevier.com/locate/ssi

The electrochemical double-layer capacitance of yttria-stabilised zirconia

M.G.H.M. Hendriks, J.E. ten Elshof*, H.J.M. Bouwmeester, H. Verweij[1]

Laboratory for Inorganic Materials Science, MESA+Research Institute, University of Twente, P.O. Box 217, 7500 AE Enschede, The Netherlands

Received 6 June 2001; received in revised form 25 September 2001; accepted 30 October 2001

Abstract

The capacitance of the double-layer at the interface between irreversible (current-blocking) gold electrodes and yttria-stabilised zirconia (YSZ) was measured by impedance spectroscopy as a function of the applied electrode potential and yttria content (2–8 mol%). At moderate temperatures, 300–660 K, the dielectric constant of zirconia stabilised with 8 mol% yttria is thermally activated with an activation energy of 12.6 ± 2.1 kJ/mol. Above 700 K, where the oxygen vacancies in YSZ are rendered mobile, contributions arise from space-charge polarisation at the blocking electrolyte/electrode interface. Based upon the Gouy–Chapman theory, a simple thermodynamic model, which takes into account the effect of site exclusion of the doubly ionised oxygen vacancies, is presented for the formed double layer. Fair agreement is obtained with the experimental differential capacitance characteristics, which show a maximum around -125 mV at 822 K. The activation energy of the dielectric constant of YSZ with 8 mol% yttria in the temperature range 700–900 K is found to be 116 ± 34 kJ/mol.

Keywords: Yttria-stabilised zirconia; Double-layer capacitance; Dielectric constant

1. Introduction

Stabilised zirconia is widely employed as the electrolyte in oxygen sensors, water electrolysers and solid oxide fuel cells, because of its high oxygen ion conductivity at elevated temperatures [1]. Despite its great technological interest, only little attention has been paid to the nature of the double layer at the metal electrode–solid oxide electrolyte interface and the magnitude of its capacitance. Determination of the latter is usually based on studies of electrode kinetics at porous metal electrodes using ac impedance spectroscopy. Corresponding results are evaluated by modelling the electrode response to an equivalent circuit consisting of linear circuit elements. Robertson and Michaels [2] have listed various equivalent circuits used in the interpretation of experimental data by different researchers, who obtained widely different values for the interface capacitance. In addition to the uncertainty over the true contact area between the porous metal electrode and the solid oxide electro-

* Corresponding author. Tel.: +31-53-4892695; fax: +31-53-4894683.

E-mail address: J.E.tenElshof@ct.utwente.nl (J.E. ten Elshof).

[1] Present address: Department of Materials Science and Engineering, The Ohio State University, Columbus, OH 43210-1178, USA.

0167-2738/02/$ - see front matter
PII: S0167-2738(01)01017-7

lyte, it is recognised that time-dependent faradaic processes may obscure the charging of the double-layer. This last effect is liable to be very important in the case of porous electrodes and makes quantitative measurement of the interface capacitance very difficult.

In this work, the capacitance at the interface between irreversible (current-blocking) gold electrodes and yttria-stabilised zirconia (YSZ) was measured by low-frequency impedance spectroscopy, as functions of electrode potential and yttria content. The experimental data are compared with theoretical predictions of the Gouy–Chapman theory [3]. In this model, the double layer is produced by the distribution of mobile oxygen vacancies in the electrolyte in the vicinity of the interface. Details of this distribution depend only on the interface potential and the defect structure. The model takes into account the effect of site exclusion, which is necessary in view of the high concentration of oxygen vacancies in stabilised zirconia. In addition, to enable quantitative comparison of the model to the experimental data, the dielectric properties of YSZ at low temperatures (<500 K) have been measured.

2. Theory

A continuum theory of the double-layer capacitance of yttria-stabilised zirconia against an inert blocking electrode is presented in this section. Following Gouy and Chapman [3], it is assumed here that under conditions of ionic equilibrium at the interface, a redistribution of the diffuse layer formed by the mobile charge carriers occurs in response to a change in the electrochemically fixed interface potential. In the model, neither size effects of ionic charge carriers nor specific adsorption at the metal–solid oxide electrolyte interface is considered.

2.1. Oxygen vacancy concentration in an electrical field

The majority mobile charge carriers in YSZ are doubly ionised oxygen vacancies. Charge neutrality requires that $[Y'_{Zr}]=2[V^{\cdot\cdot}_{O}]$, where $[Y'_{Zr}]$ is the concentration of dopant yttrium ions and $[V^{\cdot\cdot}_{O}]$ the concentration of oxygen vacancies.

The electrochemical potential of noninteracting oxygen vacancies in stabilised zirconia $\eta_{V_O^{\cdot\cdot}}$ can be expressed [4] as:

$$\eta_{V_O^{\cdot\cdot}} = \mu^0_{V_O^{\cdot\cdot}} + k_B T \ln \frac{[V^{\cdot\cdot}_O](x)}{1-[V^{\cdot\cdot}_O](x)} + q\phi(x), \tag{1}$$

where x is the distance from the electrode, $[V^{\cdot\cdot}_O]$ the molar fraction of oxygen vacancies, $\mu_{V_O^{\cdot\cdot}}{}^0$ a concentration-independent term, k_B the Boltzmann constant, q the charge on oxygen vacancies ($q=2e$, with e the elementary charge) and $\phi(x)$ the local electrical potential. Under conditions of ionic equilibrium $\eta_{V_O^{\cdot\cdot}}$ is constant and independent of location. Provided that the thickness of the diffuse double layer is small compared with the sample dimensions, the electrical potential in the bulk ($x\to\infty$) can be assumed zero. Eq. (1) can then be rearranged into:

$$[V^{\cdot\cdot}_O](x) = \frac{[V^{\cdot\cdot}_O]_{Bulk} e^{\frac{-2e\phi(x)}{k_B T}}}{1+[V^{\cdot\cdot}_O]_{Bulk}\left(e^{\frac{-2e\phi(x)}{k_B T}}-1\right)}. \tag{2}$$

The assumption made here is that $\mu_{V_O^{\cdot\cdot}}{}^0$ at the surface is not different from the value in the bulk. In view of the high defect concentration at the interface and the limited number of available lattice sites, the use of the simple Boltzmann form, which neglects site exclusion effects and is often considered for liquid electrolytes, is not appropriate for ionic solids [4].

2.2. Local electrical field in the double layer

The variation of the electrical potential in the double layer near a flat electrode/electrolyte interface satisfies Poisson's equation, which in one dimension takes the form:

$$\frac{d^2\phi(x)}{dx^2} = -4\pi\frac{\rho(x)}{\varepsilon}. \tag{3}$$

Here $\rho(x)$ is the local volume charge density and ε the dielectric constant in the space-charge layer. The

volume charge density at any point is formed by contributions from the charge carriers, i.e., oxygen vacancies and yttrium ions,

$$\rho(x) = \sum_i q_i c_i(x) = c\left(2e[\mathrm{V}_\mathrm{O}^{\cdot\cdot}](x) - e[\mathrm{Y}'_\mathrm{Zr}]\right) = 2ce\left([\mathrm{V}_\mathrm{O}^{\cdot\cdot}](x) - [\mathrm{V}_\mathrm{O}^{\cdot\cdot}]_\mathrm{Bulk}\right), \quad (4)$$

where c is the density of YSZ unit cells.

As an electrical field is absent in the bulk, the boundary condition for Eq. (3) is:

$$\lim_{x\to\infty} \frac{\mathrm{d}\phi(x)}{\mathrm{d}x} = 0. \quad (5)$$

To integrate Eq. (3) use is made of the definition of the electrical field strength $E(x)$, defined by $E(x) = -\mathrm{d}\phi(x)/\mathrm{d}x$, and,

$$\frac{\mathrm{d}^2\phi(x)}{\mathrm{d}x^2} = -\frac{\mathrm{d}E(x)}{\mathrm{d}x} = -\frac{\mathrm{d}E(x)}{\mathrm{d}\phi(x)}\frac{\mathrm{d}\phi(x)}{\mathrm{d}x} = E(x)\frac{\mathrm{d}E(x)}{\mathrm{d}\phi(x)}. \quad (6)$$

After substitution of Eqs. (4) and (2) into Eq. (3), integration of Eq. (3) yields,

$$\frac{\mathrm{d}\phi(x)}{\mathrm{d}x} = \pm\sqrt{\frac{16\pi ec}{\varepsilon}\left[[\mathrm{V}_\mathrm{O}^{\cdot\cdot}]_\mathrm{Bulk}\phi(x) + \frac{k_\mathrm{B}T}{2e}\ln\left[1 + [\mathrm{V}_\mathrm{O}^{\cdot\cdot}]_\mathrm{Bulk}\left(\mathrm{e}^{\frac{-2e\phi(x)}{k_\mathrm{B}T}} - 1\right)\right]\right]}, \quad (7)$$

where the plus or minus sign refers to (7)a negative or positive value of $\phi(0)$, respectively.

2.3. The differential capacity of YSZ

Eq. (7) cannot be solved analytically, but the surface charge density at the metal σ^M can be calculated using the Gauss theorem,

$$\sigma^\mathrm{M} = -\varepsilon\left(\frac{\mathrm{d}\phi(x)}{\mathrm{d}x}\right)_{x=0}. \quad (8)$$

The specific differential double-layer capacitance C_diff is defined as:

$$C_\mathrm{diff}(\phi) = \frac{\mathrm{d}\sigma^\mathrm{M}}{\mathrm{d}\phi}. \quad (9)$$

From Eqs. (7)–(9) it then follows that:

$$C_\mathrm{diff}(\phi_\mathrm{b}) = \mp\frac{\sqrt{4\pi\varepsilon ec}([\mathrm{V}_\mathrm{O}^{\cdot\cdot}]_\mathrm{Bulk} - [\mathrm{V}_\mathrm{O}^{\cdot\cdot}](0))}{\sqrt{[\mathrm{V}_\mathrm{O}^{\cdot\cdot}]_\mathrm{Bulk}\phi_\mathrm{b} + \frac{k_\mathrm{B}T}{2e}\ln\left[1 + [\mathrm{V}_\mathrm{O}^{\cdot\cdot}]_\mathrm{Bulk}\left(\mathrm{e}^{-\frac{2e\phi_\mathrm{b}}{k_\mathrm{B}T}} - 1\right)\right]}}, \quad (10)$$

where ϕ_b is the potential at the electrode/electrolyte interface. In Eq. (10), ε refers to the effective dielectric constant in the space-charge region near the electrode. It is emphasised here that its value may deviate substantially from the corresponding bulk dielectric constant.

The overall capacitance C_overall of a symmetrical cell with identical electrodes may be regarded as a circuit consisting of two capacitances in series. Close to zero potential difference, it follows that $C_\mathrm{overall} = 1/2C_\mathrm{diff}(0)$. The differential capacitance at zero electrode potential can be obtained by Taylor expansion of Eq. (10). This leads to:

$$C_\mathrm{overall} = 2e\sqrt{\frac{\pi\varepsilon c}{k_\mathrm{B}T}[\mathrm{V}_\mathrm{O}^{\cdot\cdot}]_\mathrm{Bulk}(1 - [\mathrm{V}_\mathrm{O}^{\cdot\cdot}]_\mathrm{Bulk})}. \quad (11)$$

3. Experimental

Commercial yttria-stabilised zirconia powders (Tosoh, Tokyo, Japan), denoted as TZ-2Y, TZ-3Y and TZ-8Y for samples containing 2, 3 and 8 mol% yttria, respectively, were pressed into pellets under 400 MPa. The TZ-2Y and TZ-3Y pellets were sintered over 98% dense in air at 1400 °C for 4 h, while the TZ-8Y pellet was sintered over 99% dense at 1480 °C for 2 h. Prior to use, the disks were polished using a 3 μm diamond emulsion.

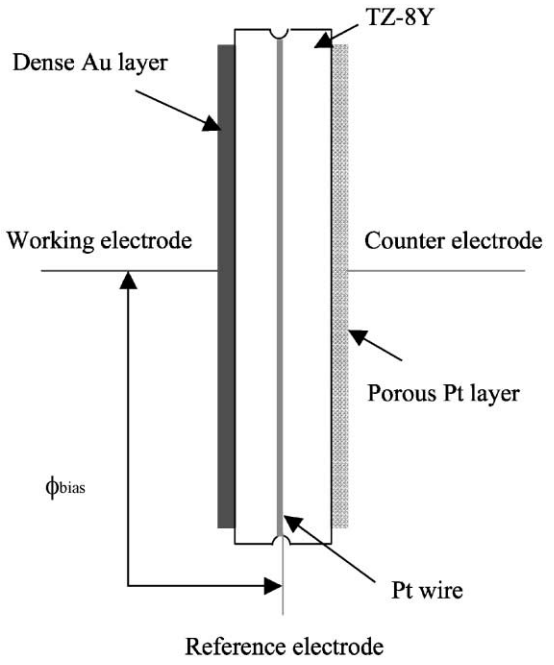

Fig. 1. Schematic picture of the experimental set-up for differential capacitance measurements.

For differential capacitance measurements the YSZ pellets were cut into discs (Ø 16.0 mm; thickness 4.0 mm). A circular notch was carved into the cylindrical side of the disc. Around the notch a platinum wire, serving as the reference electrode, was attached using platinum paste. One of the flat surfaces was painted with platinum paste to serve as the counter electrode. The platinum electrode was fired in air at 1200 °C and then cooled down slowly. The Pt electrode was porous after this pre-treatment. The opposite flat surface was sputtered with a dense gold layer to serve as the working electrode.

A schematic drawing of the cell is shown in Fig. 1. Measurements were performed under a nitrogen atmosphere at a temperature of 822 K. The potential difference between the working and reference electrode was varied between −250 and +50 mV using a potentiostat (Potentiostat LB 75L, Bank Elektronik, Göttingen, Germany). Three-point impedance measurements were performed using a frequency response analyser (Solartron Instruments 1250 FRA, Schlumberger Technologies, Farnborough, Hampshire, England) at 10 mV rms in the frequency range of 10 mHz to 60 kHz. The experimental impedance dispersion curves were fitted to an equivalent circuit consisting of a constant phase element (CPE) and a resistance in series using the Equivalent Circuit software program [5]. The differential capacitance at zero frequency was calculated from the CPE values.

For dielectric constant and overall capacitance measurements, the compacts were cut into disks of 13.5 mm diameter and 2.0 mm thickness. A dense gold layer was sputtered on both sides; two-point impedance measurements were carried out in the temperature range 298–873 K and the same frequency range as used in the differential capacitance measurements.

4. Results and discussion

Results from two-point impedance measurements at room temperature are shown in Table 1. The relative dielectric constants ε_r were determined from the high frequency behaviour (>1 kHz) using the standard expression for the geometric capacitance $C = \varepsilon_0 \varepsilon_r A/d$, where ε_0 is the permittivity of vacuum, ε_r is the bulk dielectric constant, and A and d are the geometric surface area and thickness of the capacitor, respectively. The tetragonal zirconia samples (2 and 3 mol% yttria) show the highest relative dielectric constant, while the cubic zirconia sample (8 mol% yttria) has a slightly lower value. Thompson et al. [6] measured the relative dielectric constants of monoclinic, tetragonal and cubic zirconia, stabilised with different concentrations of various ions. Some of their results are listed in Table 1 for comparison. The values found in both studies for 3 mol% yttria-stabilised zirconia are in close agreement. Thompson et al. [6] suggested that the relative dielectric constant is determined primarily by the crystallographic form, rather than by the nature or

Table 1
Dielectric constants of yttria-stabilised zirconia with varying yttria content; $T = 298$ K; $f = 1–60$ kHz

Mol% Y_2O_3	Structure	ε_r; experimental	ε_r; Thompson et al. [6]
0	monoclinic	–	23.0
2	tetragonal	40.5	–
3	tetragonal	39.5	39.5
6	tetragonal	–	39.0
8	cubic	28.7	–

amount of the dopant. The results obtained in the present study support this suggestion.

The temperature dependence of the relative dielectric constant of cubic zirconia (TZ-8Y), calculated with the same expression as above from high frequency measurements, is shown in Fig. 2. A logarithmic dependence on temperature can be clearly seen. The activation energy of ε_r is equal to 12.6 ± 2.1 kJ/mol. The magnitude of the activation energy is reasonably close to the value of approximately 19.2 kJ/mol reported by Jonscher and Reau [7] for the relative dielectric constant of lead fluoride.

The results from overall capacitance measurements performed at 822 K are listed in Table 2. In qualitative agreement with the model predictions, the capacitance increases with yttria dopant concentration. From Eq. (11), a capacitance C_{norm}, normalised with respect to the bulk concentration of oxygen vacancies, can be defined:

$$C_{\mathrm{norm}} = \frac{C_{\mathrm{overall}}}{\sqrt{[\mathrm{V}_{\mathrm{O}}^{\cdot\cdot}]_{\mathrm{Bulk}}(1-[\mathrm{V}_{\mathrm{O}}^{\cdot\cdot}]_{\mathrm{Bulk}})}} = 2e\sqrt{\frac{\pi\varepsilon c}{k_{\mathrm{B}}T}}. \quad (12)$$

The results listed in Table 2 show that these normalised capacitances have comparable values within

Table 2
Overall capacitances in YSZ with varying yttria content; $T = 822$ K; $f < 10$ Hz

Mol% Y_2O_3	C_{overall} [F m^{-2}]	C_{norm} [F m^{-2}]
2	0.80 ± 0.13	8.1 ± 1.3
3	1.29 ± 0.21	10.8 ± 1.7
8	1.63 ± 0.26	8.6 ± 1.4

experimental error. This indicates that the dielectric constants in the double-layers have roughly the same value.

Overall capacitance measurements were performed on TZ-8Y in the temperature interval 700–900 K. At temperatures above approximately 700 K yttria-stabilised zirconia becomes significantly oxygen ion-conducting, and is therefore capable of forming a double-layer capacitance. At temperatures higher than 900 K, the gold electrodes started to sinter, leading to irreproducible results. Fig. 3 shows the increase of the overall capacitance with temperature. Eq. (11) was fitted to the experimental data using the relative dielectric constant as a fit parameter. In contrast with the high frequency data shown in Fig. 2, the low-frequency (< 1 Hz) measurements show a different activation energy for the relative dielectric constant (116 ± 34 kJ/mol). This is due to the fact that the activation energy for the dielectric constant contains

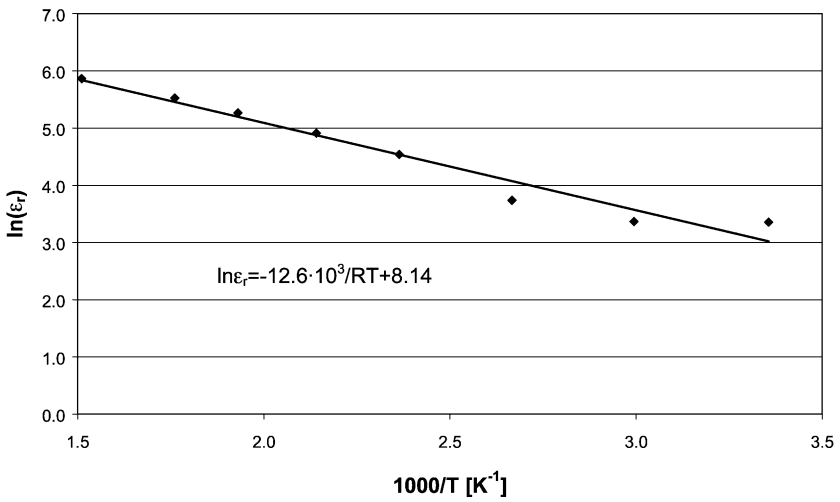

Fig. 2. Experimental dielectric constant of TZ-8Y as a function of temperature; $f > 1$ kHz.

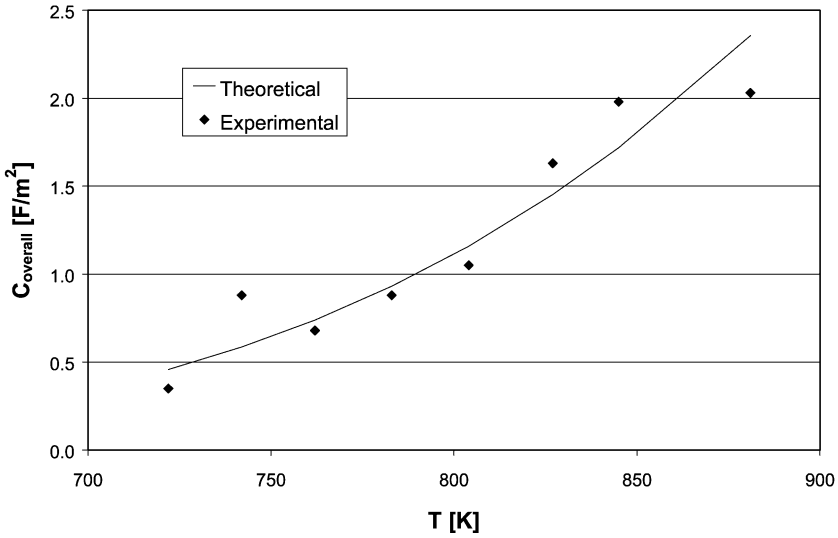

Fig. 3. Experimental and theoretical overall capacitances in TZ-8Y as a function of temperature; $f < 100$ Hz.

an additional thermally activated component that is due to space-charge polarisation.

In Fig. 4, the experimental differential capacitances of TZ-8Y at 822 K are shown as a function of electrode bias potential. The trend predicted by Eq. (10) is also shown. The experimental data at $\phi_b = 0$ were fitted to Eq. (10). This yielded a value $\varepsilon_r \sim 1$ for the relative dielectric constant in the double-layer region. As is observed here, the value of the dielectric constant in the double-layer is significantly smaller than the bulk dielectric constant [8]. The qualitative agreement between the experimental and theoretically predicted curves in Fig. 4 is reasonable. With decreasing bias potential the experimental differential

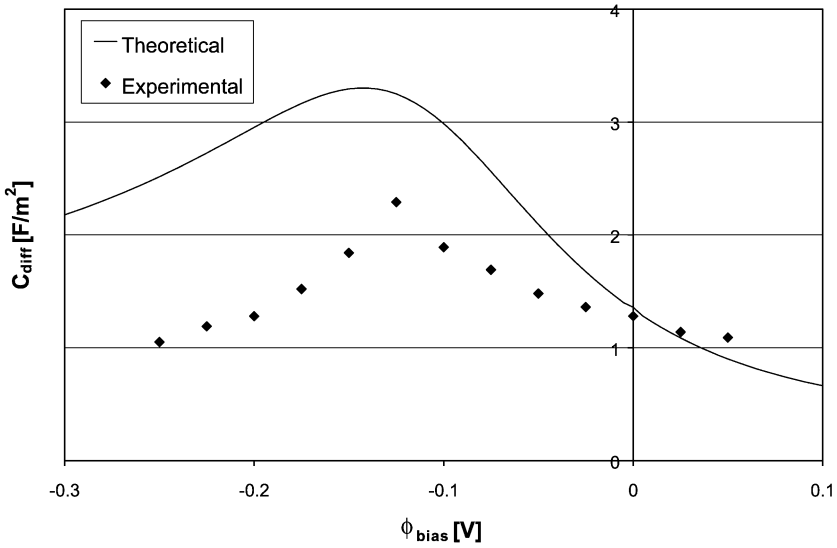

Fig. 4. Experimental and theoretical differential capacitances in TZ-8Y as function of bias potential; $T = 822$ K; $f < 100$ Hz.

capacitance reaches a maximum value at approximately −125 mV, which is reasonably close to the maximum of −143 mV predicted by the model. For the experimental data and theoretical calculations, similar slopes are obtained near the maximum. In view of Eq. (9), a maximum in the differential capacitance will occur at the bias potential ϕ_C at which the surface charge σ^M changes most rapidly with changing potential. To a first order of approximation, this potential coincides with the electrode bias potential at which the oxygen vacancy concentration $[V_O^{\cdot\cdot}]$ at the interface changes most rapidly with bias potential, i.e., where $(d^2[V_O^{\cdot\cdot}]/d\phi^2)=0$. From Eq. (2) it can be derived that:

$$\phi_C \approx -\frac{k_B T}{2e}\ln\left(\frac{1-[V_O^{\cdot\cdot}]_{Bulk}}{[V_O^{\cdot\cdot}]_{Bulk}}\right). \quad (13)$$

Using this approximation, $\phi_C \approx -115$ mV for TZ-8Y at 822 K. It should be noted that Robertson and Michaels [2], who measured the differential double-layer capacitance at an interface between a porous platinum electrode and YSZ at 828–968 K, did not observe a bias potential dependency of the differential capacitance.

The model proposed here assumes that every oxygen site in the lattice will be occupied by an oxygen vacancy when the bias potential is sufficiently low. On the other hand, it can be seen in Fig. 4 that the experimental $C_{diff}(\phi_b)$ values are smaller than the theoretical ones for all $\phi_b<0$. As Eq. (9) can be rewritten into:

$$\sigma_M = \int_0^{\phi_b} C_{diff}(\phi)\,d\phi, \quad (14)$$

it follows that less surface charge σ_M is present on the surface in reality than predicted by the model for $\phi_b<0$. And since σ_M is counterbalanced by an equally large ionic charge in the double-layer, the actual oxygen vacancy concentration in the double-layer must be lower than predicted. Hence, the model overestimates the concentration of oxygen vacancies in the double-layer.

5. Conclusions

At room temperature, the relative dielectric constant of yttria-stabilised zirconia compacts with varying amounts of yttria depends on the crystal structure. Tetragonal zirconia has the highest value (~ 40), while the value for cubic zirconia is ~ 29. In the temperature interval 300–660 K, the dielectric constant of cubic zirconia appears to be thermally activated (12.6 ± 2.1 kJ/mol).

At temperatures above 700 K, where the oxygen vacancies are mobile, contributions arise from space-charge polarisation at the blocking electrolyte/electrode interface. The overall capacitance was found to increase with increasing oxygen vacancy concentration. The results agree reasonably well with model predictions based upon Gouy–Chapman theory. The differential capacitance reached a maximum at −125 mV, which is close to the value predicted by the model. The activation energy of the dielectric constant in the temperature interval 700–900 K was 116 ± 34 kJ/mol. The discrepancy between model predictions and experimental data at negative bias potentials indicates that not all oxygen sites in the lattice can be occupied by vacancies, which was one of the underlying assumptions in the derivation of the model.

Acknowledgements

Assistance in performing the experiments by R.J. Greven is gratefully acknowledged.

References

[1] H.J.M. Bouwmeester, A.J. Burggraaf, in: P.J. Gellings, H.J.M. Bouwmeester (Eds.), The CRC Handbook of Solid State Electrochemistry, CRC Press, Boca Raton, 1997, pp. 481–553.
[2] N.L. Robertson, J.N. Michaels, J. Electrochem. Soc. 1385 (1991) 1494.
[3] A.J. Bard, L.R. Faulkner, Electrochemical Methods: Fundamentals and Applications, Wiley, New York, 1980, p. 488.
[4] M.H.R. Lankhorst, Thermodynamic and transport properties of mixed ionic–electronic conducting perovskite-type oxides, PhD thesis, University of Twente, Enschede, 1997.
[5] B.A. Boukamp, Solid State Ionics 20 (1986) 31.
[6] D.P. Thompson, A.M. Dickins, J.S. Thorp, J. Mater. Sci. 27 (1992) 2267.
[7] A.K. Jonscher, J.M. Réau, J. Mater. Sci. 13 (1978) 563.
[8] K. Natori, D. Otani, N. Sano, Appl. Phys. Lett. 73 (1998) 632.